Scripta Materialia 157 (2018) 95–99

Contents lists available at ScienceDirect

Scripta Materialia

journal homepage: www.elsevier.com/locate/scriptamat

Regular article

The roles of internal and external hydrogen in the deformation and fracture processes at the fatigue crack tip zone of metastable austenitic stainless steels

Yuhei Ogawa [a,b,*], Saburo Okazaki [c,d], Osamu Takakuwa [d,e,g], Hisao Matsunaga [d,e,f,g]

[a] Graduate School of Engineering, Kyushu University, 744 Motooka, Nishi-ku, Fukuoka 819-0395, Japan
[b] Research Fellow of the Japan Society for the Promotion of Science, 744 Motooka, Nishi-ku, Fukuoka 819-0395, Japan
[c] Kobe Material Testing Laboratory Co., Ltd., 47-13 Niijima, Harima-cho, Kako-gun, Hyogo 675-0155, Japan
[d] Research Center for Hydrogen Industrial Use and Storage (HYDROGENIUS), Kyushu University, 744 Motooka, Nishi-ku, Fukuoka 819-0395, Japan
[e] Department of Mechanical Engineering, Kyushu University, 744 Motooka, Nishi-ku, Fukuoka 819-0395, Japan
[f] International Institute for Carbon-Neutral Energy Research (I2CNER), Kyushu University, 744 Motooka, Nishi-ku, Fukuoka 819-0395, Japan
[g] AIST-Kyushu University Hydrogen Materials Laboratory (HydroMate), 744 Motooka, Nishi-ku, Fukuoka 819-0395, Japan

ARTICLE INFO

Article history:
Received 10 July 2018
Accepted 3 August 2018
Available online xxxx

Keywords:
Hydrogen embrittlement
Fatigue
Austenitic steels
Martensitic phase transformation

ABSTRACT

Fatigue crack growth (FCG) tests were performed with two types of metastable austenitic stainless steels having different austenite phase stabilities under hydrogen-precharged conditions (internal hydrogen) and in gaseous hydrogen environments (external hydrogen). The materials showed a peculiarly slower FCG rate with internal hydrogen than with external hydrogen even though the hydrogen concentration was much higher under the internal hydrogen conditions. The results are interpreted in terms of hydrogen-modified plastic deformation character comprising inhibited cross-slipping or enhanced deformation twinning in combination with the sequence of hydrogen penetration and strain-induced α′ martensite formation in the local region surrounding the fatigue crack tip.

Austenitic stainless steels are widely used as components in recent high-pressure hydrogen applications, such as pipes and valves for fuel cell vehicles (FCVs) or hydrogen refueling stations, due to their superior resistance to hydrogen embrittlement. However, when the stability of austenite phase is relatively low, the materials sometimes suffer from dramatic hydrogen-induced degradation of the mechanical performance under plastic deformation, which is generally attributed to the strain-induced α′ martensitic transformation [1–7]. This embrittlement phenomenon in metastable austenitic stainless steels related to a plasticity-induced phase transformation is considered especially problematic in fatigue crack growth (FCG) processes since severe plastic deformation in the crack tip zone essentially forms martensite, even in materials with a relatively high austenite stability [8–12]. During the past few decades, numerous studies have been conducted to elucidate the precise mechanism of interaction between the phase transformation in the crack tip zone, dissolved hydrogen and the resultant FCG acceleration; however, a decisive conclusion has not yet been achieved because of the complex nature of the mechanism.

One possible contributor that complicates the interpretation of such a well-known fact is that the setups for FCG experiments, *i.e.*, the specimen configuration, load ratio, and test frequency, have not been consistent in previous studies [8,9,12,13]. Furthermore, another significant problem is that some of those experiments were performed under different hydrogen supplying conditions, such as under hydrogen-precharged conditions [8–10] or in a gaseous hydrogen environment [12,13], which are frequently termed as "internal" and "external" hydrogen, respectively. In austenitic steels, in which the diffusivity of hydrogen is significantly low at ambient temperature [14,15], hydrogen atoms can penetrate from the surface to a depth on the order of only μm when the materials are mechanically tested in a gaseous hydrogen environment [4]. Accordingly, in tensile testing, hydrogen-induced degradation is generally mitigated with external hydrogen compared with hydrogen-precharged conditions, *i.e.*, when hydrogen is uniformly supplied inside the material prior to testing [4]. However, this typical trend is sometimes reversed, especially in FCG tests of metastable austenitic stainless steels [9,12,13]. In fact, a significant acceleration of FCG was reported for Type 304 steels in a hydrogen atmosphere, even at relatively low pressures [12,13], whereas precharging with approximately 100 wt ppm hydrogen conversely decelerated FCG in the same material [9]. This experimental evidence indicates that FCG tests conducted with large amounts of internal hydrogen can possibly provide

* Corresponding author at: Graduate School of Engineering, Kyushu University, 744 Motooka, Nishi-ku, Fukuoka 819-0395, Japan.
E-mail address: yuhei.ogawa.205@kyudai.jp (Y. Ogawa).

https://doi.org/10.1016/j.scriptamat.2018.08.003
1359-6462/

a nonconservative interpretation. Therefore, the cause of such a peculiar contradiction should be thoroughly understood to assess the hydrogen compatibility of metastable austenitic stainless steels from the viewpoint of the FCG resistance.

In this study, we present critical experimental results for screening the influences of internal and external hydrogen on the FCG acceleration behavior of metastable austenitic stainless steels under a universal experimental setup, *i.e.*, identical specimen configuration, load ratio, test frequency, temperature and stress intensity factor range. The combined techniques of electron backscatter diffraction (EBSD) analysis and electron channeling contrast imaging (ECCI) were successfully applied to the crack paths to elucidate the individual roles of internal and external hydrogen in plastic deformation, phase transformation and fracture processes in the crack tip zone.

Solution-annealed plates of two types of metastable austenitic stainless steels with different austenite stabilities, *i.e.*, AISI Type 304 and 316L steels, were used in this study. The chemical compositions, nickel equivalent values (Ni_{eq}), which is an index for evaluating the austenite phase stability [16], and mechanical properties of these materials are summarized in Table 1. The compact-tension (CT)-type specimens with a width W of 50.8 mm and thickness B of 10.0 mm were cut from the L-T orientation of the plate materials. FCG tests were performed in laboratory air and a hydrogen gas environment with pressures of 0.7 and 90 MPa at room temperature (RT) according to the ASTM-E647 standard [17] under a constant stress intensity factor range, ΔK, of 30 MPa $m^{1/2}$. As the tests with internal hydrogen, some of the specimens of each material were precharged with hydrogen by exposing them to 100 MPa of hydrogen gas at 270 °C for 780 h and then tested in air. Based on the literature data for the hydrogen diffusivity in austenitic stainless steels, this hydrogen-charging condition is enough to obtain a uniform hydrogen distribution throughout the specimen thickness [14]. A load range, R, of 0.1 and testing frequency, f, of 1 Hz were selected for all of the FCG experiments. After FCG testing, the CT specimens were cut along the mid-thickness sections and carefully polished with diamond pastes and colloidal SiO_2 to remove the damaged surface layer. The crack paths were analyzed using EBSD and ECCI *via* a field-emission scanning electron microscope (FE-SEM) operated at 15–20 kV to visualize the phase transformation and corresponding deformation substructures. Additionally, blocks with dimensions of 10 × 10 × 10 mm were fabricated from the corners of the hydrogen-precharged CT specimens, and the hydrogen content was measured *via* thermal desorption analysis (TDA).

Fig. 1 shows the FCG acceleration rate measured in the presence of internal and external hydrogen relative to that measured in their absence and the estimated hydrogen concentration, C_S, under each environmental condition. The C_s in the external hydrogen tests represents the surface hydrogen concentration in the gaseous state, and for the internal hydrogen tests, it represents the saturated concentration of the equilibrium state achieved by precharging, which was simply calculated by Sievert's law according to the hydrogen solubility data of the same materials [14]. The C_S values were estimated to be approximately 4 and 60 wt ppm in 0.7 and 90 MPa of hydrogen gas, respectively, and 90 wt ppm under the hydrogen-precharged condition. The TDA measurements of the hydrogen-precharged specimens confirmed that their practical hydrogen contents were almost consistent with the estimated C_S values in both materials. On the other hand, note that values in the case of external hydrogen, the estimated C_S values are just the local

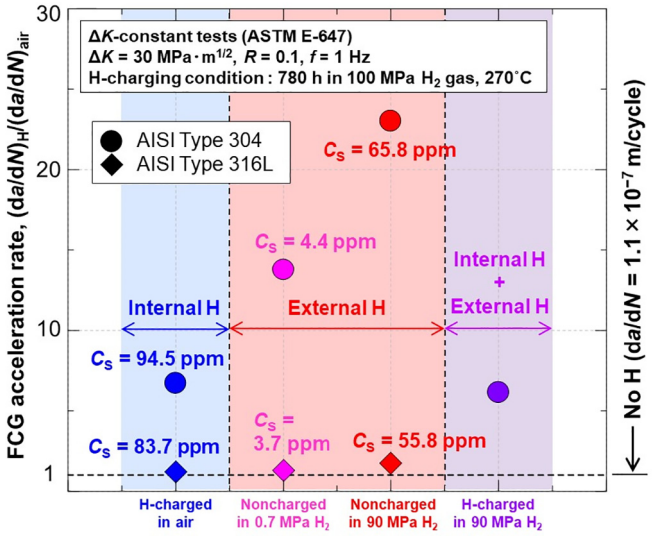

Fig. 1. FCG acceleration rates of Type 304 and 316L austenitic stainless steels in gaseous hydrogen environments and under hydrogen-precharged conditions relative to those in the absence of hydrogen. (For interpretation of the references to color in this figure, the reader is referred to the web version of this article.)

hydrogen concentrations in the crack tip zone, assuming that the crystal phase in that zone is still austenite. Since the material at the crack tip locally transforms into martensite, which has a low hydrogen solubility, the practical hydrogen concentrations at the crack tip under 0.7 and 90 MPa of hydrogen gas are expected to be much smaller than the values indicated in Fig. 1.

Due to its high austenite stability, Type 316L steel showed almost no FCG acceleration under all testing conditions. Conversely, significant acceleration was confirmed for Type 304 steel with both internal and external hydrogen. For external hydrogen, the FCG rate showed higher values at higher gas pressures, *i.e.*, 14- and 23-fold acceleration at 0.7 and 90 MPa, respectively, which is supposedly due to the larger hydrogen concentration. However, the more noteworthy result in Fig. 1 is the considerably lower acceleration rate, *i.e.*, 7 times, observed in the hydrogen-precharged specimen. Even though this specimen contained more than 90 wt ppm hydrogen, its acceleration rate was almost half as much as the case of 0.7 MPa hydrogen gas that can provide only a few wt. ppm or less of hydrogen in the crack tip zone.

Fig. 2 presents the crystal orientation maps and corresponding phase maps around the mid-thickness crack paths in Type 304 steel analyzed *via* EBSD. Severe cyclic plastic strain caused a large degree of α′ transformation with the size of approximately 10~30 μm in the absence of hydrogen (Fig. 2 (d)), whereas in 90 MPa hydrogen gas, the transformed region was highly localized in the crack path (Fig. 2 (e)). As indicated in Fig. 2 (e) and (f), hydrogen facilitated cracking along both the α′ phase interior and/or the α′/γ interfaces. This α′-related hydrogen-induced cracking phenomenon usually leads to the formation of a quasi-cleavage type fracture surface, which is proposed to be responsible for hydrogen-induced FCG acceleration in metastable austenitic stainless steels [12,18]. Here, we deduce that the abovementioned localization of the α′ phase is a consequence of faster and successive cracking

Table 1
Chemical compositions and nickel equivalent, Ni_{eq}, values (wt%) of the materials used in this study together with the yield stress, σ_y, and ultimate tensile stress, σ_B (MPa).

Material	C	Si	Mn	P	S	Ni	Cr	Mo	Ni_{eq}	σ_y	σ_B
Type 304	0.06	0.42	0.84	0.030	0.002	8.09	18.16	–	22.8	274	628
Type 316L	0.018	0.50	0.84	0.021	0.000	12.09	17.45	2.05	27.5	229	528